

# Crystal structure of the one-dimensional dihalide-bridged polymer dibromobis(thiazole)nickel(II) by powder neutron diffraction

Michael James

Neutron Scattering Group, Australian Nuclear Science and Technology Organisation (ANSTO), Lucas Heights Research Laboratories, PMB 1, Menai N.S.W. 2234, Australia

The polymeric compound  $\text{Ni}(\text{tz})_2\text{Br}_2$  ( $\text{tz} = 1,3\text{-thiazole}$ ) has been synthesized by the addition of thiazole to an ethanolic solution of anhydrous  $\text{NiBr}_2$ . Powder X-ray and neutron diffraction measurements were used for structural determination. An attempt to solve the structure using powder X-ray diffraction data was unsuccessful due to the presence of unrefinable preferred orientation, a consequence of the needle-like nature of the microcrystalline powder. The structure was determined using powder neutron diffraction data and Rietveld techniques: space group  $I2/a$ ,  $a = 17.8854(7)$ ,  $b = 3.7705(2)$ ,  $c = 15.0919(7)$  Å,  $\beta = 92.0007(3)^\circ$ ,  $U = 1017.13(8)$  Å<sup>3</sup>,  $Z = 4$ . The structure consists of pseudo-octahedral units, doubly linked by halide bridges to form infinite linear chains.

Polymeric systems based on transition metals, thiazole (tz) and dibridging halide ligands have been known for some time;<sup>1,2</sup> however, the structure of dichlorobis(thiazole)copper(II) was previously the only one to have been reported.<sup>3</sup> The recent study of the crystal structures of  $\text{Fe}(\text{tz})_2\text{Cl}_2$  and  $\text{Cu}(\text{tz})_2\text{Br}_2$  by single crystal techniques<sup>4</sup> added to the structural information on this class of compounds, but highlighted the difficulty in growing suitable single crystals of these and indeed most polymer complexes. These compounds are normally obtained as powdered materials and are typically insoluble in common organic solvents and therefore difficult to crystallise. With advances in laboratory X-ray powder diffractometers and by use of *ab initio* and Rietveld techniques, a number of crystal structures of polymer complexes have been solved from powder diffraction data. Masciocchi *et al.* have in the past few years demonstrated that the crystal structures of polymer complexes such as  $[\text{Ni}(\text{pydz})\text{X}_2]$  (pydz = pyridazine; X = Cl or Br),<sup>5</sup>  $[\text{M}(\text{pz})]$  (M = Ag or Cu; Hpz = pyrazole)<sup>6</sup> and  $[\text{M}(4,4'\text{-bipy})\text{X}_2]$  (M = Ni or Cu; X = Cl or Br)<sup>7</sup> could be successfully determined using these methods. This study describes the synthesis of the polymer  $\text{Ni}(\text{tz})_2\text{Br}_2$  and its structural characterisation using powder diffraction and Rietveld techniques.

## Experimental

Anhydrous  $\text{NiBr}_2$  (98% purity) and thiazole (99% purity) were obtained from Aldrich Chemical Co. Inc. Ethanol (A. R. grade) was used when freshly distilled. Elemental analyses were carried out on a LECO CHNS-900 elemental analyser. Infrared spectra were recorded (Nujol mull) in the 350–5200  $\text{cm}^{-1}$  range on a Perkin-Elmer FT-IR 2000 spectrophotometer.

### Preparation of $\text{Ni}(\text{tz})_2\text{Br}_2$

Thiazole (12 mmol, 2 ml) was added to an ethanolic solution of anhydrous  $\text{NiBr}_2$  (6 mmol, 16 ml) with constant stirring. A yellow precipitate was formed from a green solution. The sample was stirred for 10 min, collected, washed with diethyl ether and benzene and allowed to dry under suction [Found: C, 18.3; H, 1.6; N, 6.9; S, 16.8. Calc. for  $\text{Ni}(\text{tz})_2\text{Br}_2$ : C, 18.5; H, 1.6; N, 7.2; S, 16.5%]. IR (Nujol):  $\nu(\text{ligand})$  609s, 635w, 739s, 808s, 882m, 917m, 1067m, 1110m, 1237m and 1320m  $\text{cm}^{-1}$ .

### Powder diffraction

Powder X-ray diffraction measurements were made on a Rigaku *ttaxs*  $\theta/\theta$  rotating anode X-ray diffractometer at

ambient temperature using Cu-K $\alpha$  radiation and a flat-plate sample holder. Data of sufficient quality for structural refinement were collected over the range  $5 < 2\theta < 85^\circ$ , in  $0.02^\circ$  steps, with integration times of 10 s. Powder neutron diffraction measurements were made on the high resolution powder diffractometer (HRPD) instrument<sup>8</sup> using thermal neutrons ( $\lambda = 1.8825$  Å) from the high flux Australian reactor (HIFAR) nuclear reactor at ANSTO<sup>9</sup> and a vanadium sample can. Data were collected using a bank of 24 <sup>3</sup>He detectors over the range  $0.86 < 2\theta < 154^\circ$ , in  $0.05^\circ$  steps. Structural refinements were carried out by the Rietveld method<sup>10</sup> using the LHPM program,<sup>11</sup> with pseudo-Voigt peak shapes and an interpolated background.

## Results and Discussion

The chemical reactivity of nickel(II) bromide with thiazole appears to be slightly different to that observed for copper(II) halides.<sup>1–4</sup> Reactions based on copper(II) halides produce only polymeric  $\text{Cu}(\text{tz})_2\text{X}_2$  (X = Cl or Br) compounds, while reactions based on nickel(II) halides have been shown to produce both the monomeric species  $\text{Ni}(\text{tz})_4\text{Br}_2$  as well as the polymeric compound  $\text{Ni}(\text{tz})_2\text{Br}_2$ . In this respect the nickel-based materials show similar reactivity to those of the cobalt(II) halides.<sup>1,2</sup>

### X-Ray crystallography

Fig. 1 shows the X-ray diffraction profile of  $\text{Ni}(\text{tz})_2\text{Br}_2$ . Attempts to index this diffraction pattern based on the monoclinic  $P2_1/c$  cell of  $\text{Cu}(\text{tz})_2\text{Br}_2$  [ $a = 7.460(2)$ ,  $b = 3.987(3)$ ,

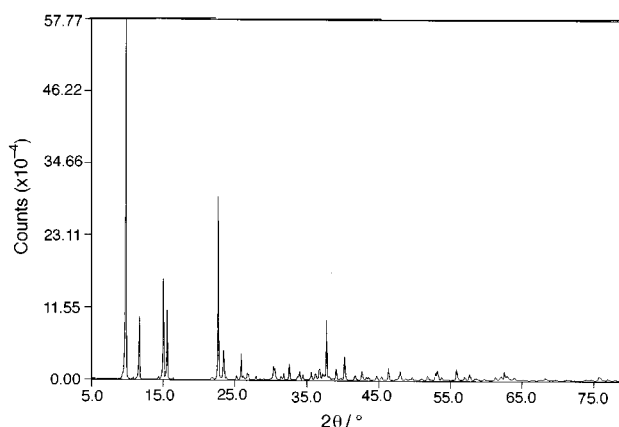
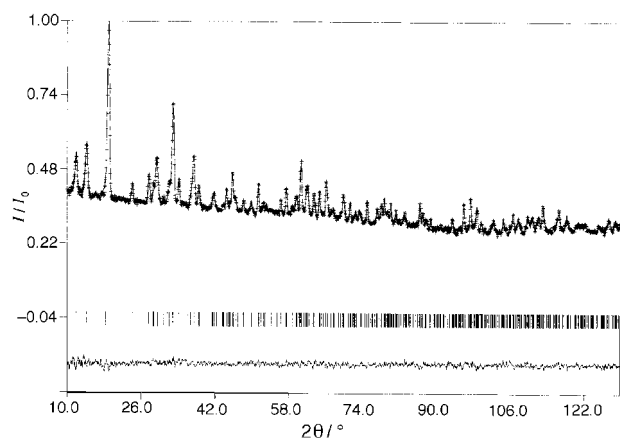


Fig. 1 Observed powder X-ray diffraction profile for  $\text{Ni}(\text{tz})_2\text{Br}_2$

**Table 1** Crystallographic (powder neutron diffraction) data for Ni(tz)<sub>2</sub>Br<sub>2</sub>

Formula	C <sub>6</sub> H <sub>6</sub> Br <sub>2</sub> N <sub>2</sub> NiS <sub>2</sub>
<i>M</i>	388.74
Space group	<i>I</i> 2/a (no. 15)
<i>a</i> /Å	17.8854(7)
<i>b</i> /Å	3.7705(2)
<i>c</i> /Å	15.0919(7)
β/°	92.007(3)
<i>U</i> /Å <sup>3</sup>	1017.13(8)
<i>Z</i>	4
2θ Range/°	10.0–130.0
No. of reflections	505
Goodness of fit	0.7
<i>R</i> <sub>p</sub> / <i>R</i> <sub>B</sub> (%)	1.6, 7.9



**Fig. 2** Observed (points), calculated (full line) and difference powder neutron diffraction patterns for Ni(tz)<sub>2</sub>Br<sub>2</sub>

*c* = 17.757(2) Å, β = 92.15(1)°, *Z* = 2] or the *Cc* cell of Fe(tz)<sub>2</sub>Cl<sub>2</sub> [*a* = 17.908(9), *b* = 3.717(5), *c* = 14.870(8) Å, β = 95.30(5)°, *Z* = 4]<sup>4</sup> were unsuccessful. More satisfactory indexing was achieved in the monoclinic *I*2/a space group, with cell parameters similar to those observed for Fe(tz)<sub>2</sub>Cl<sub>2</sub><sup>4</sup> (see Table 1). The initial model used for the Rietveld refinement of the structure was based on a similar dibridging polymeric arrangement to that shown for Fe(tz)<sub>2</sub>Cl<sub>2</sub>, from which a poor fit to these data was obtained (*R*<sub>p</sub> = 42.7, *R*<sub>B</sub> = 42.4%). Refinement of the Dollase preferred orientation function<sup>12</sup> along the (010) direction did lead to an improvement in the fit to these data (*R*<sub>p</sub> = 19.8, *R*<sub>B</sub> = 16.8%). The large value of the March coefficient (1.76) supports the notion of the microcrystalline powder being composed of needle-like particles, this being consistent with the macroscopic forms taken by single-crystal samples of Cu(tz)<sub>2</sub>X<sub>2</sub> (*X* = Cl<sup>3</sup> or Br<sup>4</sup>) and Fe(tz)<sub>2</sub>Cl<sub>2</sub>.<sup>4</sup> Free refinement of the non-hydrogen fractional coordinates further improved the fit (*R*<sub>p</sub> = 17.5, *R*<sub>B</sub> = 11.3%), however examination of the resultant structure revealed significant 'non-physical' distortion of the planar thiazole rings. Difficulties associated with structural determination using flat-plate Bragg–Brentano powder X-ray diffraction data result from the inability successfully to model the substantial preferred orientation.

### Neutron crystallography

The same initial model was adopted for the Rietveld refinement of the structure using powder neutron diffraction data. Upon refinement of the atomic positions and isotropic thermal parameters, an excellent fit to these data was obtained despite the high background that resulted from incoherent scattering from the hydrogen present in the sample. The crystallographic data obtained from the refinement of the structure using powder neutron diffraction data are given in Table 1, while the refined atomic coordinates and isotropic thermal parameters

**Table 2** Fractional atomic coordinates and equivalent isotropic thermal parameters (*B*<sub>eq</sub>) for Ni(tz)<sub>2</sub>Br<sub>2</sub> with estimated standard deviations in parentheses

Atom	<i>x</i>	<i>y</i>	<i>z</i>	<i>B</i> <sub>eq</sub> <sup>a</sup> /Å <sup>2</sup> × 100
Ni	0.75	0.330(2)	0.00	1.3(1)
Br	0.6875(4)	0.824(2)	−0.0971(4)	1.6(1)
N	0.8429(3)	0.332(1)	−0.0810(3)	1.4(1)
S	0.9176(7)	0.352(4)	−0.2117(9)	0.9(2)
C1	0.8349(3)	0.368(2)	−0.1669(4)	1.6(1)
C2	0.9675(4)	0.282(2)	−0.1179(5)	2.2(1)
C3	0.9146(3)	0.275(2)	−0.0542(4)	1.8(1)
H1	0.7851(9)	0.420(4)	−0.1984(9)	3.6(3)
H2	1.0246(9)	0.242(5)	−0.1135(9)	4.4(4)
H3	0.9242(8)	0.247(5)	0.0257(9)	4.0(4)

$$^a B_{eq} = (8/3)\pi^2[U_{11}(aa^*)^2 + U_{22}(bb^*)^2 + U_{33}(cc^*)^2 + 2U_{12}aa^*bb^*\cos\gamma + 2U_{13}aa^*cc^*\cos\beta + 2U_{33}bb^*cc^*\cos\alpha]$$

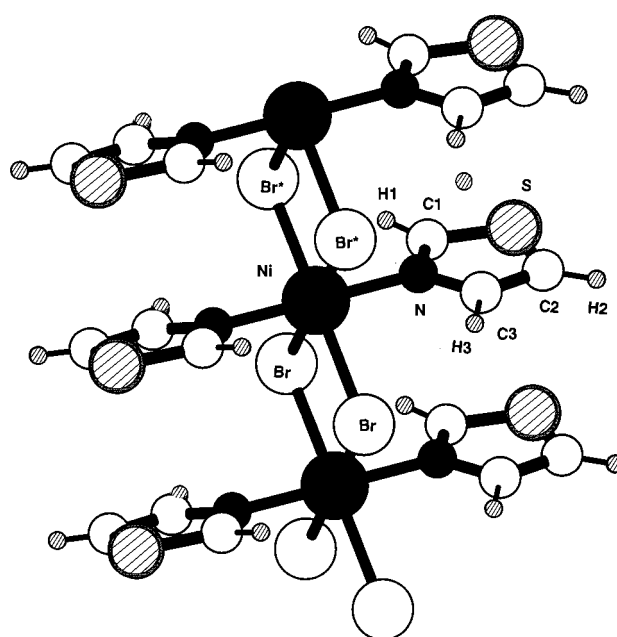


**Fig. 3** The one-dimensional polymer structure of Ni(tz)<sub>2</sub>Br<sub>2</sub>, with the chain direction along the *b* axis

are given in Table 2. The observed and calculated neutron diffraction profiles for Ni(tz)<sub>2</sub>Br<sub>2</sub> are shown in Fig. 2. Examination of Fig. 2 reveals a number of weak peaks (e.g. ≈16.3, 21.3 and 22.3°) that could not be indexed using this unit cell which are believed to result from Ni(tz)<sub>4</sub>Br<sub>2</sub>. As no crystal structure has been reported for Ni(tz)<sub>4</sub>Br<sub>2</sub> this phase was not able to be fitted in the profile refinement.

### Crystal structure of Ni(tz)<sub>2</sub>Br<sub>2</sub> 1

The structure of Ni(tz)<sub>2</sub>Br<sub>2</sub> consists of tetragonally elongated octahedral units, with N-donor thiazole ligands in the axial positions. These units are equatorially linked along the *b* axis by double bromide bridges to form infinite linear chains (Fig. 3). The packing of these chains in the unit cell is shown in Fig. 4. Selected bond lengths and bond angles are given in Table 3. The polymeric compound consists of the same dihalide bridged linear structure as has been found for Cu(tz)<sub>2</sub>X<sub>2</sub> (*X* = Cl<sup>3</sup> or Br<sup>4</sup>) and Fe(tz)<sub>2</sub>Cl<sub>2</sub>.<sup>4</sup> The Ni<sub>2</sub>Br<sub>2</sub> structural motif based on dibridging bromide ligands has also been observed in a number of other dimeric<sup>13–17</sup> and polymeric<sup>5,7</sup> nickel(II) complexes. The polymer [M(4,4'-bipy)Br<sub>2</sub>]<sup>7</sup> in particular shows essentially isostructural co-ordination features to Ni(tz)<sub>2</sub>Br<sub>2</sub> with a *trans* arrangement of Ni–N bonds and dibridging Br–Ni–Br\* bonds. The Ni–N distance in Ni(tz)<sub>2</sub>Br<sub>2</sub> of 2.097(5) Å is consistent with those values [2.083(5)–2.184(4) Å] observed for other Ni–N

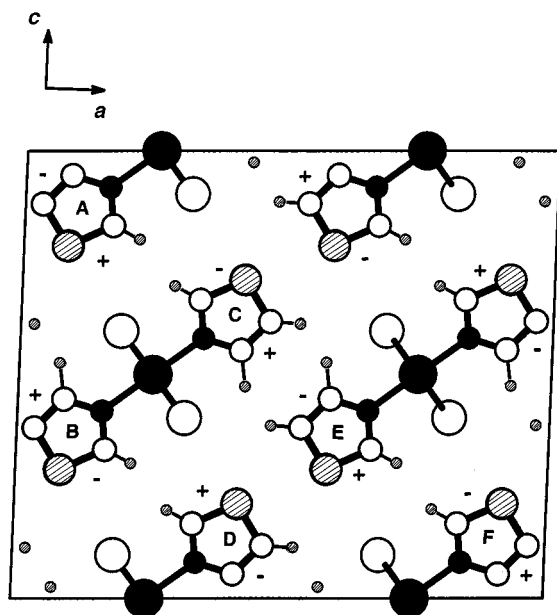


Fig. 4 Packing of infinite linear chains in the unit cell of  $\text{Ni}(\text{tz})_2\text{Br}_2$ . The chain direction is into the page (parallel to the  $b$  axis)

Table 3 Selected bond lengths ( $\text{\AA}$ ) and angles ( $^\circ$ ) for  $\text{Ni}(\text{tz})_2\text{Br}_2$

$\text{Ni} \cdots \text{Ni}^{*a}$	3.771(1)		
$\text{Ni}-\text{Br}$	2.631(8)	$\text{C1}-\text{S}$	1.65(1)
$\text{Ni}-\text{Br}^*$	2.598(8)	$\text{S}-\text{C2}$	1.67(1)
$\text{Ni}-\text{N}$	2.097(5)	$\text{C2}-\text{C3}$	1.373(9)
$\text{N}-\text{Cl}$	1.306(8)	$\text{C3}-\text{N}$	1.348(8)
$\text{C1}-\text{H1}$	1.01(2)	$\text{C2}-\text{H2}$	1.03(2)
$\text{C3}-\text{H3}$	1.22(2)		
$\text{Br}-\text{Ni}^*-\text{Br}$	87.0(1)	$\text{Ni}-\text{Br}-\text{Ni}^*$	92.3(1)
$\text{Br}-\text{Ni}-\text{Br}$	88.4(2)	$\text{Br}-\text{Ni}^*-\text{Br}^*$	92.3(1)
$\text{N}-\text{Ni}-\text{N}^*$	179.7(2)	$\text{Br}-\text{Ni}-\text{Br}^*$	179.3(2)
$\text{Br}-\text{Ni}-\text{N}$	90.4(2)	$\text{Br}^*-\text{Ni}-\text{N}$	89.8(2)
$\text{Ni}-\text{N}-\text{Cl}$	121.1(5)	$\text{Ni}-\text{N}-\text{C3}$	126.2(6)
$\text{C1}-\text{N}-\text{C3}$	122.6(6)	$\text{N}-\text{C3}-\text{C2}$	117.3(5)
$\text{C2}-\text{S}-\text{C1}$	96.8(8)	$\text{C3}-\text{C2}-\text{S}$	103.6(8)
$\text{S}-\text{Cl}-\text{N}$	109.6(8)		

<sup>a</sup> An asterisk denotes a translation of the molecule along the  $b$  axis.

bonded systems of this type.<sup>5,7</sup> The  $\text{Ni}-\text{Br}$  bond lengths in  $\text{Ni}(\text{tz})_2\text{Br}_2$  of 2.598(8) and 2.631(8)  $\text{\AA}$  are also in agreement with values (2.458–2.641  $\text{\AA}$ ) observed for other complexes containing the  $\text{Ni}_2\text{Br}_2$  structural motif.<sup>5,7,13–17</sup> Moreover, the majority of these complexes display a similar degree of  $\text{Ni}-\text{Br}$  bond asymmetry ( $\approx 0.03$   $\text{\AA}$ ) within each  $\text{Ni}_2\text{Br}_2$  unit. The bond angles  $\text{Br}-\text{Ni}-\text{Br}^*$ ,  $\text{Br}-\text{Ni}-\text{N}$  and  $\text{N}-\text{Ni}-\text{N}$  (Table 3) show little deviation away from regular octahedral geometry.

The dimensions of the thiazole ligand of  $\text{Ni}(\text{tz})_2\text{Br}_2$  are typical of those found in other metal thiazole complexes.<sup>3,4,18–20</sup> These axial thiazole ligands show opposed rotations about their  $\text{Ni}-\text{N}$  bonds with respect to the  $ac$  plane. The thiazole rings labeled B and C in Fig. 4 for example are rotated approximately  $17^\circ$  with respect to one another. The sense of tilting of the thiazole rings in Fig. 4 is indicated such that atoms labeled '+' are positioned above the  $ac$  plane, while '-' atoms are positioned below.

Closer examination of  $\text{Ni}(\text{tz})_2\text{Br}_2$  indicates slightly different structural behaviour to that observed in  $\text{Cu}(\text{tz})_2\text{Br}_2$ ,<sup>4</sup> suggesting dissimilar bonding mechanisms. In contrast to the opposed rotational behaviour of the thiazole rings in  $\text{Ni}(\text{tz})_2\text{Br}_2$  (Figs. 3 and 4), the rings in  $\text{Cu}(\text{tz})_2\text{Br}_2$  show synchronised rotations about their  $\text{Cu}-\text{N}$  bonds of approximately  $21^\circ$  relative to the  $ac$  plane. These distinct rotational behaviours are clearly linked to the different transition metal-halide bonding modes in these

Table 4 Selected interchain distances ( $\text{\AA}$ ) for  $\text{Ni}(\text{tz})_2\text{Br}_2$

Ring	Atom	Ring	Atom	Interchain distance
A	H1	C	H1	2.35(2)
C	H2	E	H3	2.43(2)
D	H2		H3	2.50(2)
E	H2		Br	2.93(2)
A	H1		Br	3.29(2)
D	S	E	H2	3.22(2)
D	H1	E	S	3.68(2)
D	S	E	S	3.72(2)

complexes. The polymer structure of  $\text{Cu}(\text{tz})_2\text{Br}_2$  can be described as a square-planar array consisting of two thiazole ligands and two short in-plane bromide bonds [2.472(1)  $\text{\AA}$ ] linked by the two longer out-of-plane  $\text{Cu}-\text{Br}$  bonds [3.120(1)  $\text{\AA}$ ]. This distortion of the pseudo-octahedral bonding arrangement is reflective of the Jahn–Teller nature of the  $d^9 \text{Cu}^{2+}$ . The tilting of the thiazole ring in this complex tends to be towards the longer of the two  $\text{Cu}-\text{Br}$  bonds to the relief of steric pressure in the structure.<sup>4</sup> The bonding picture about the nickel centre of  $\text{Ni}(\text{tz})_2\text{Br}_2$  on the other hand reveals a more regular pseudo-octahedral co-ordination. The square-planar-like arrangement observed for  $\text{Cu}(\text{tz})_2\text{Br}_2$  is inappropriate here, where only slight variation is shown between the  $\text{Ni}-\text{Br}$  bonds; hardly surprising, given that Jahn–Teller effects do not contribute significantly to the  $d^8$  ground state configuration of  $\text{Ni}^{2+}$ .

Both  $\text{Ni}(\text{tz})_2\text{Br}_2$  and  $\text{Fe}(\text{tz})_2\text{Cu}_2$ <sup>4</sup> crystallise in unit cells of approximately the same size; twice that of  $\text{Cu}(\text{tz})_2\text{X}_2$  ( $\text{X} = \text{Cl}^3$  or  $\text{Br}^4$ );  $\text{Ni}(\text{tz})_2\text{Br}_2$  may further be distinguished from the iron and copper complexes by the packing arrangement of the polymer chains within the crystal. The tilting of thiazole rings and the placement of the transition metal centres gives rise to an  $I$ -centred arrangement, while a  $C$ -centred disposal is found for  $\text{Fe}(\text{tz})_2\text{Cl}_2$ .<sup>4</sup> While  $\text{Ni}(\text{tz})_2\text{Br}_2$  and  $\text{Fe}(\text{tz})_2\text{Cl}_2$ <sup>4</sup> each show opposed tilting across the transition metal centres, the nearest-neighbour interchain interactions differ. In the case of  $\text{Ni}(\text{tz})_2\text{Br}_2$  each of the nearest-neighbour interactions occur between thiazole rings with opposite tilts with respect to the  $ac$  plane (Table 4). Atom H1 on ring A for example is tilted above the  $ac$  plane, while H1 on ring C is tilted below the plane; H2 and H3 on rings C and E show similar relationships. For  $\text{Fe}(\text{tz})_2\text{Cl}_2$ ,<sup>4</sup> the analogous  $\text{H1} \cdots \text{H1}$  interaction shows the same behaviour as in  $\text{Ni}(\text{tz})_2\text{Br}_2$ , however the analogous  $\text{H2} \cdots \text{H3}$  interactions differ in that both rings are tilted below the  $ac$  plane.

Although the tilting of the thiazole ligands leads to different interchain interactions, the nature of these connections remains essentially the same. It should be noted that despite the presence of the larger bromine atoms, the nearest interchain distances for  $\text{Ni}(\text{tz})_2\text{Br}_2$  (Table 4) are smaller than those observed for the chloride-based systems.<sup>3,4</sup>

## Acknowledgements

I wish to acknowledge the assistance of Dr. B. A. Hunter in the collection of the neutron diffraction data, as well as Dr. S. J. Kennedy for his helpful discussions.

## References

- M. N. Hughes and K. J. Rutt, *J. Chem. Soc. A*, 1970, 3015.
- W. J. Eilbeck, F. Holmes and A. E. Underhill, *J. Chem. Soc. A*, 1967, 757.
- W. E. Estes, D. P. Gavel, W. E. Hatfield and D. J. Hodgson, *Inorg. Chem.*, 1978, **17**, 1415.
- M. James, H. Kawaguchi and K. Tatsumi, *Polyhedron*, 1998, **17**, 1843.
- N. Masciocchi, P. Cairati, L. Carlucci, G. Ciani, G. Mezza and A. Sironi, *J. Chem. Soc., Dalton Trans.*, 1994, 3009.
- N. Masciocchi, M. Moret, P. Cairati, A. Sironi, G. A. Ardizzoia and G. La Monica, *J. Am. Chem. Soc.*, 1994, **116**, 7668.

- 7 N. Masciocchi, P. Cairati, L. Carlucci, G. Mezza, G. Ciani and A. Sironi, *J. Chem. Soc., Dalton Trans.*, 1996, 2739.
- 8 C. J. Howard, C. J. Ball, R. L. Davis and M. M. Elcombe, *Aust. J. Phys.*, 1983, **36**, 507.
- 9 S. J. Kennedy, *Adv. X-Ray Anal.*, 1995, **38**, 35.
- 10 H. M. Rietveld, *J. Appl. Crystallogr.*, 1969, **2**, 65.
- 11 C. J. Howard and B. A. Hunter, LHPM, A Computer Program for Rietveld Analysis of X-ray and Neutron Powder Diffraction Patterns, Australian Nuclear Science and Technology Organisation, Menai, 1997.
- 12 W. A. Dollase, *J. Appl. Crystallogr.*, 1986, **18**, 267.
- 13 P. L'Haridon and I. Bkouche-Waksman, *J. Inorg. Nucl. Chem.*, 1978, **40**, 2025.
- 14 G. B. Jameson, H. R. Oswald and H. R. Beer, *J. Am. Chem. Soc.*, 1984, **106**, 1669.
- 15 G. Guerch, P. Mauret, J. Jaud and J. Galy, *Acta Crystallogr., Sect. B*, 1977, **33**, 3747.
- 16 R. J. Butcher and E. Sinn, *Inorg. Chem.*, 1977, **16**, 2334.
- 17 U. Thewalt, R. Hemmer and H. A. Brune, *Z. Naturforsch., Teil B*, 1979, **34**, 859.
- 18 M. James, H. Kawaguchi and K. Tatsumi, *Polyhedron*, 1997, **16**, 1873.
- 19 M. James, H. Kawaguchi and K. Tatsumi, *Polyhedron*, 1997, **16**, 4279.
- 20 M. James, H. Kawaguchi and K. Tatsumi, *Acta Crystallogr., Sect. C*, 1997, **53**, 1391.

Received 8th June 1998; Paper 8/04338H